

LA-UR-21-30173

Accepted Manuscript

The Role of Oxygen Transfer in Oxide Heterostructures on Functional Properties

Corey, Zachary John
Han, Hyungkyu
Kang, Kyeong Tae
Wang, Xuejing
Paudel, Binod
Roy, Pinku
Sharma, Yogesh
Yoo, Jinkyong
Jia, Quanxi
Chen, Aiping

Provided by the author(s) and the Los Alamos National Laboratory (2022-05-20).

To be published in: Advanced Materials Interfaces

DOI to publisher's version: 10.1002/admi.202101867

Permalink to record:

<http://permalink.lanl.gov/object/view?what=info:lanl-repo/lareport/LA-UR-21-30173>



Los Alamos National Laboratory, an affirmative action/equal opportunity employer, is operated by Triad National Security, LLC for the National Nuclear Security Administration of U.S. Department of Energy under contract 89233218CNA000001. By approving this article, the publisher recognizes that the U.S. Government retains nonexclusive, royalty-free license to publish or reproduce the published form of this contribution, or to allow others to do so, for U.S. Government purposes. Los Alamos National Laboratory requests that the publisher identify this article as work performed under the auspices of the U.S. Department of Energy. Los Alamos National Laboratory strongly supports academic freedom and a researcher's right to publish; as an institution, however, the Laboratory does not endorse the viewpoint of a publication or guarantee its technical correctness.

The Role of Oxygen Transfer in Oxide Heterostructures on Functional Properties

*Zachary Corey, Henry H. Han, Kyeong Tae Kang, Xuejing Wang, Rebecca A. Lalk, Binod Paudel, Pinku Roy, Yogesh Sharma, Jinkyoungh Yoo, Quanxi X. Jia, * Aiping Chen **

Z. Corey, P. Roy, Prof. Q. X. Jia

Department of Materials Design and Innovation, University at Buffalo - The State University of New York, Buffalo, NY 14260, USA

E-mail: qxjia@buffalo.edu

Z. Corey, Dr. H. H. Han, Dr. K. T. Kang, Dr. X. Wang, R. Lalk, B. Paudel, P. Roy, Dr. Y. Sharma, Dr. J. Yoo, Dr. A. Chen

Center for Integrated Nanotechnologies (CINT), Los Alamos National Laboratory, Los Alamos, New Mexico 87545, USA

E-mail: apchen@lanl.gov

B. Paudel

Department of Physics, New Mexico State University, Las Cruces, NM 88001, USA

Dr. H.H. Han

Current address: Energy and Environment Directorate, Pacific Northwest National Laboratory, Richland, Washington 99352, USA

KEYWORDS: epitaxial growth, oxide heterostructures, oxygen transfer, high mobility, oxygen vacancy, thin films

This is the author manuscript accepted for publication and has undergone full peer review but has not been through the copyediting, typesetting, pagination and proofreading process, which may lead to differences between this version and the [Version of Record](#). Please cite this article as [doi: 10.1002/admi.202101867](https://doi.org/10.1002/admi.202101867).

Abstract: A variety of mechanisms are reported to play critical roles in contributing the high carrier/electron mobility in oxide/SrTiO₃ (STO) heterostructures. By using La_{0.95}Sr_{0.05}TiO₃ (LSTO) epitaxially grown on different single crystal substrates (such as STO, GdScO₃, LaAlO₃, (LaAlO₃)_{0.3}(Sr₂AlTaO₆)_{0.7}, and CeO₂ buffered STO) as the model systems, we show that the formation of a conducting substrate surface layer (CSSL) on STO substrate at relatively low growth temperature and high oxygen pressure (725 °C, 5 × 10⁻⁴ Torr) contributes to the enhanced conductivity of the LSTO/STO heterostructures. Different from conventional oxygen vacancy model, our work reveals that the formation of the CSSL occurs when growing an oxide layer (LSTO in this case) on STO, while neither annealing nor the growth of a Au layer alone at the exact same growth condition generates the CSSL in STO. It demonstrates that the oxide layer actively pulls oxygen from STO substrate at given growth conditions, leading the formation of the CSSL. Our observations emphasize the oxygen transfer across film/substrate interface during the synthesis of oxide heterostructures play critical roles on functional properties.

Author Manuscript

1. Introduction

Strain, defects and interface play critical roles in controlling functional properties in a variety of oxide heterostructures and nanocomposites.^[1, 2] High carrier mobility and high conductivity achieved by interfacing two insulating oxides have attracted great attention in the past decade.^[3-10] Different conduction mechanisms including polar catastrophe (interface),^[5, 10, 11] strain,^[12-14] intermixing (doping),^[3, 8, 15-17] and oxygen vacancy (defect)^[18-21] have been proposed to explain such phenomenon. For example, carriers at the substrate-film interface (interface), bulk part of the film (film) and the surface layer of the substrate near the substrate-film interface (substrate surface layer) can all contribute to the effective conductivity of the samples. Polar catastrophe is a well-established model to explain the high conductivity at the interface between LaAlO₃ and SrTiO₃ (LAO/STO).^[5, 11, 20] High mobility has also been reported when LaTiO₃ (LTO) and La_{1-x}Sr_xTiO₃ (LSTO) are grown on SrTiO₃ (STO)^[8, 14, 16, 22] and KTaO₃ (KTO).^[6] LTO is a polar perovskite like LAO, and as such, polar catastrophe mechanisms of this system are assumed to follow similarly to that of LAO/STO heterostructures.^[5, 11, 20] However, unlike LAO, which is a band insulator, LTO is a Mott insulator that shows an insulator-metal transition when doped with Sr²⁺ in polycrystalline bulk and epitaxial thin films. This allows the 3d¹ configuration to approach 3d⁰ and may also result in the observed metallic behavior as reported in LSTO films on (LaAlO₃)_{0.3}(Sr₂AlTaO₆)_{0.7} (LSAT) substrates.^[17, 23]

In addition, defects such as oxygen vacancy (OV) in the STO substrate is another factor which could affect the electric conductivity in STO-based heterostructures. The formation of OV in STO substrate is directly controlled by growth temperature and oxygen pressure as reported in different oxide/STO heterostructures.^[5, 15, 18, 20, 21, 23-28] Enhanced conductivity is observed for these heterostructures grown (and STO single crystals annealed) in temperatures greater than 750 °C, in oxygen pressure lower than 10⁻⁵ Torr or a combination of both.^[29] For example, OVs can be introduced by reducing the STO substrate with pre-substrate annealing (PSA) at 750 °C and 10⁻⁶ Torr.^[28] Spinelli, *et al.* reported highly conductive STO crystals annealed at 10⁻⁹ Torr and 700 °C.^[29]

This article is protected by copyright. All rights reserved.

Schneider *et al.* found substantial oxygen transfer from STO substrates to oxide films while studying the diffusion of isotope ^{18}O at the condition of $750\text{ }^\circ\text{C}$ and 1×10^{-8} Torr.^[19] Edmondson *et al.* observed STO substrate reduction at $10^{-10} \sim 10^{-7}$ Torr and $700\text{ }^\circ\text{C}$.^[20] Therefore, the formation of OV near STO surface or the diffusion of oxygen out from STO is driven by the relatively higher temperature (e.g., $>750\text{ }^\circ\text{C}$) and low oxygen pressure (e.g., $<1\times 10^{-5}$ Torr). Lower temperatures or higher oxygen pressures often results in insulating or significantly lowered conductivity. Post-growth annealing in oxygen rich environments can produce highly resistive films by significantly reducing the OVs.^[3, 5, 12, 15, 16, 20, 21, 30]

Except OVs directly induced by growth condition (relatively high temperature/low oxygen pressure), there are other reduction mechanisms including Ar-ion bombardment,^[31] plasma plume,^[27] and unintentional chamber contamination.^[25] UV radiation from the PLD plasma plume was found to increase OV formation as compared to the STO substrates in the same vacuum condition without UV radiation,^[26] and plume species were also observed to trigger redox-reactions for LAO/STO heterostructures.^[27] Creating oxygen vacancies in STO substrates has also been investigated by reducing STO substrate with the use of Ar-ion bombardment for LAO/STO films.^[21] The Hall mobility of Ar-ion bombarded STO was found to be the same as LAO/STO films grown at low oxygen pressures, and low oxygen pressure annealed STO substrate alone showed nearly the same sheet resistivity as LAO/STO prepared under the same growth conditions.

Although conduction mechanisms based on polar catastrophe and OV in LAO/STO systems are well studied,^[5, 15, 20, 21, 32] the origin of OV is less clear.^[6, 8, 10, 14, 19, 20, 33] The generation of OV is often believed to be due to the low oxygen growth pressure at high growth temperatures.^[19-21] However, the oxygen transfer between the oxide substrate and oxide layer could be linked to OV origin.^[19, 20, 33] In this work, we have used $\text{La}_{0.95}\text{Sr}_{0.05}\text{TiO}_3$ (LSTO) films as a platform to reveal the role of oxygen transfer during heterostructure synthesis on conductivity of the systems. We selected LSTO because it 1) has a similar structure to STO; and 2) has significant lower mobility than STO. We study the roles of substrate, processing oxygen pressure, thickness and heterointerface on the

conductivity of LSTO based heterostructures. We have isolated the contributions from the film layer, substrate and film-substrate interface separately, and concluded that the enhanced conductivity in our LSTO/STO heterostructures are due to the formation of a conducting substrate surface layer (CSSL) near STO top surface. To understand the formation mechanism of the CSSL, Au/STO reference samples were synthesized at the same growth conditions as LSTO/STO. Interestingly, our results demonstrated that this CSSL is not directly driven by processing condition alone (It is well accepted that STO losses oxygen at high temperature and low oxygen processing condition), rather it is formed because the growth of the oxide layer (LSTO in this case) actively pulls oxygen from STO substrate at the given growth condition. Our results offer a new understanding on OV formation during thin film growth via oxygen transfer mechanisms and can be applied for the growth of a variety of complex oxide films.

Author Manuscript

2. Results and Discussion

As shown in **Figure 1a**, the shifting of (002) diffraction angle of LSTO peaks on different substrates indicates different levels of in-plane strain. This is expected given the lattice mismatch between the bulk LSTO ($a \sim 3.958 \text{ \AA}$)^[23, 34] and the substrates LAO ($a = 3.792 \text{ \AA}$, -4.32%), LSAT ($a = 3.868 \text{ \AA}$, -2.53%), STO ($a = 3.905 \text{ \AA}$, -1.39%) and GSO ($a = 3.961 \text{ \AA}$, 0.08%). The biaxial lattice strain along the *c*-axis for LSTO/LSAT, LSTO/LAO, LSTO/STO and LSTO/GSO are 0.72%, 0.65%, 0.26% and nearly strain free, respectively. The lattice mismatch between the LSTO and the GSO is negligible and leads to the overlap of (002) LSTO diffraction with the GSO substrate peak. Figure 1b shows a typical reciprocal space map (RSM) near STO (103) peak. It shows that the LSTO film is probably fully strained in-plane to the STO substrate. The epitaxial relationships based on X-ray diffraction (XRD) analysis can be described as $(001)_{\text{LSTO}} \parallel (001)_{\text{Substrate}}$ and $[110]_{\text{LSTO}} \parallel [110]_{\text{Substrate}}$. The HRTEM image in Figure 1d shows the sharp interface of the LSTO film on STO substrate. The columnar structure is seen above a few tens of nanometers, indicating that the growth deviates from the 2D epitaxial growth. The formation of zig-zag or pyramid like topological feature could be due to the lower surface energy, which is also reported in TiO_2 .^[35] It is noted that the diffraction pattern shown in the inset of Figure 1c also confirms the epitaxial growth of the film and the orientation relationship between the film and the substrate.

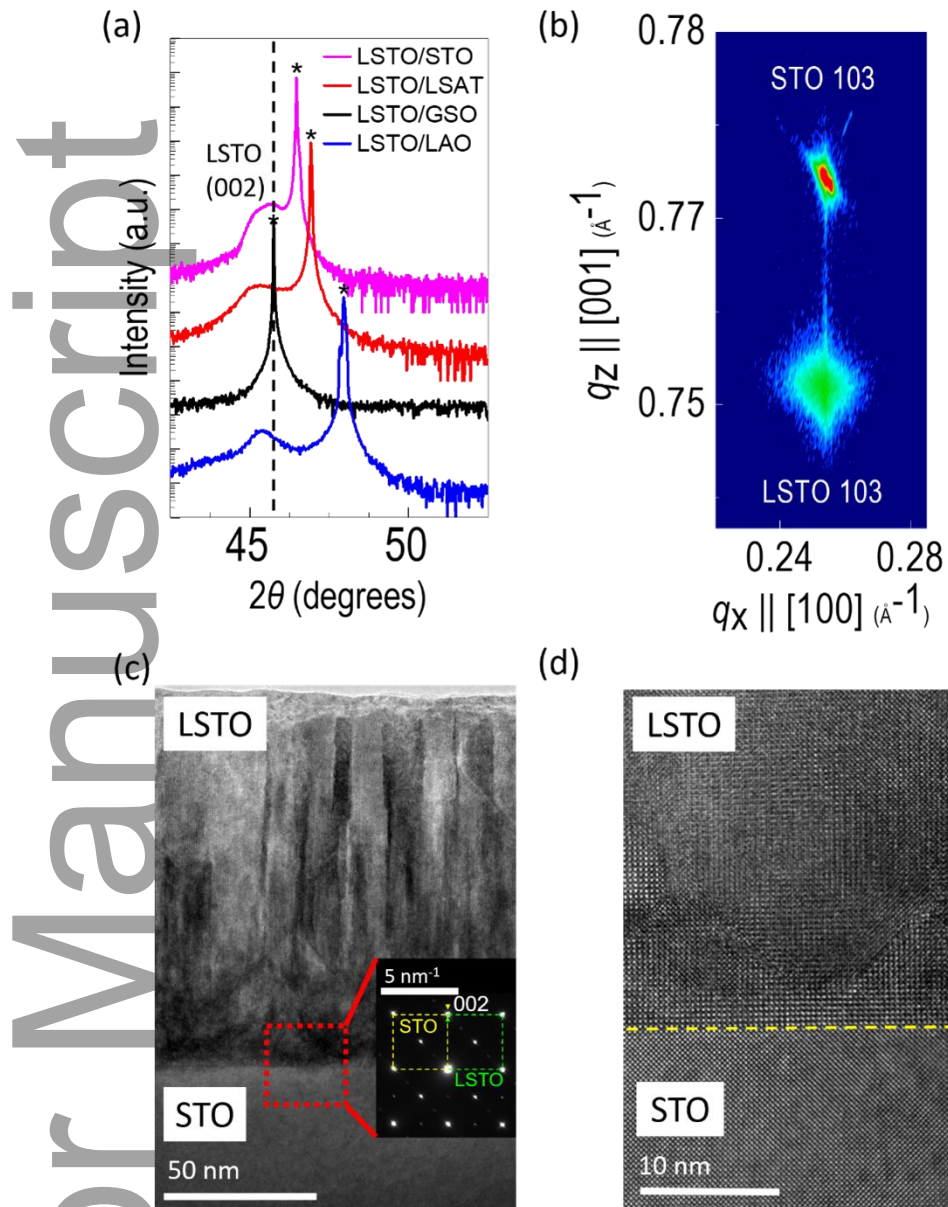


Figure 1. (a) θ - 2θ scans of 28 nm LSTO films grown on different substrates around diffractions of (110) GSO, (001) LSAT, (001) LAO and (001) STO. Substrate peaks are marked as * and the dashed line indicates location of (002) LSTO with negligible strain. (b) RSM for 122 nm LSTO film on STO near diffractions of (103) of the film and the substrate. (c) Transmission electron microscopy (TEM) image of 122 nm LSTO/STO heterostructure, where the inset shows selected area electron diffraction pattern. (d) High resolution TEM (HRTEM) image across the interface between LSTO and STO.

Figure 2a shows the ρ - T curves for 28 nm LSTO films on different substrates, where the overall temperature dependent resistivity for LSTO on LAO, LSAT and GSO are similar to the reported results.^[17, 23, 36, 37] A resistivity value around $10^{-4} \sim 10^{-3} \Omega \text{ cm}$ for our LSTO films (on LAO, LSAT and GSO) grown at an oxygen pressure of 5×10^{-4} Torr is consistent with the reported data.^[17, 23] However, different from previous reported p -type conductivity of $\text{La}_{1-x}\text{Sr}_x\text{TiO}_3$ ($0 < \text{Sr} < 0.1$) films, LSTO films in this work grown on different substrates exhibit n -type conductivity. The mobility of the LSTO films ranges from $0.1 \sim 1 \text{ cm}^2/\text{V-s}$ and carrier concentration is about 10^{22} cm^{-3} (as shown in Figures 2b and 2c). The growth of LSTO films at low oxygen partial pressure in our experiment may promote the formation of n -type conductivity due to OV, similar to the reported results for STO and TiO_2 .^[4] Since these three different substrate materials are insulating even subjected to the low oxygen pressure environment at high growth temperature, the resistivity illustrated in Figure. 2(a) should be from the LSTO films only.

Interestingly, the LSTO/STO heterostructure shows a much lower resistivity as shown in Figure 2a, and this significant change cannot be explained by the lattice strain. Figure 2b shows that

carrier concentration is approximately the same for all samples. On the other hand, the LSTO/STO stack exhibits much higher mobility as shown in Figure 2c. It is also noted that the high mobility of LSTO/STO stack and its temperature dependence of μ - T characteristic are similar to the results of an amorphous LAO layer on STO substrate and reduced STO.^[18, 21, 31, 38] Since the resistivity of reduced STO is one magnitude lower than that of LSTO at room temperature and 3-4 orders of magnitude lower at 10 K, it is clear that the resistivity in LSTO/STO stack is dominated by the more conductive STO substrate and/or the LSTO/STO interface. To exclude the interfacial contribution from the LSTO/STO heterostructure, we also inserted a CeO₂ (5 – 10 nm) layer between LSTO and STO. Our experimental results showed that CeO₂ interlayer has no obvious effect on the mobility and slightly reduces the carrier concentration below 200 K (**Figure S1**). This clearly indicates that the interface between the LSTO and the STO is not critical to achieve enhanced conductivity, different from the LAO/STO case.^[5]

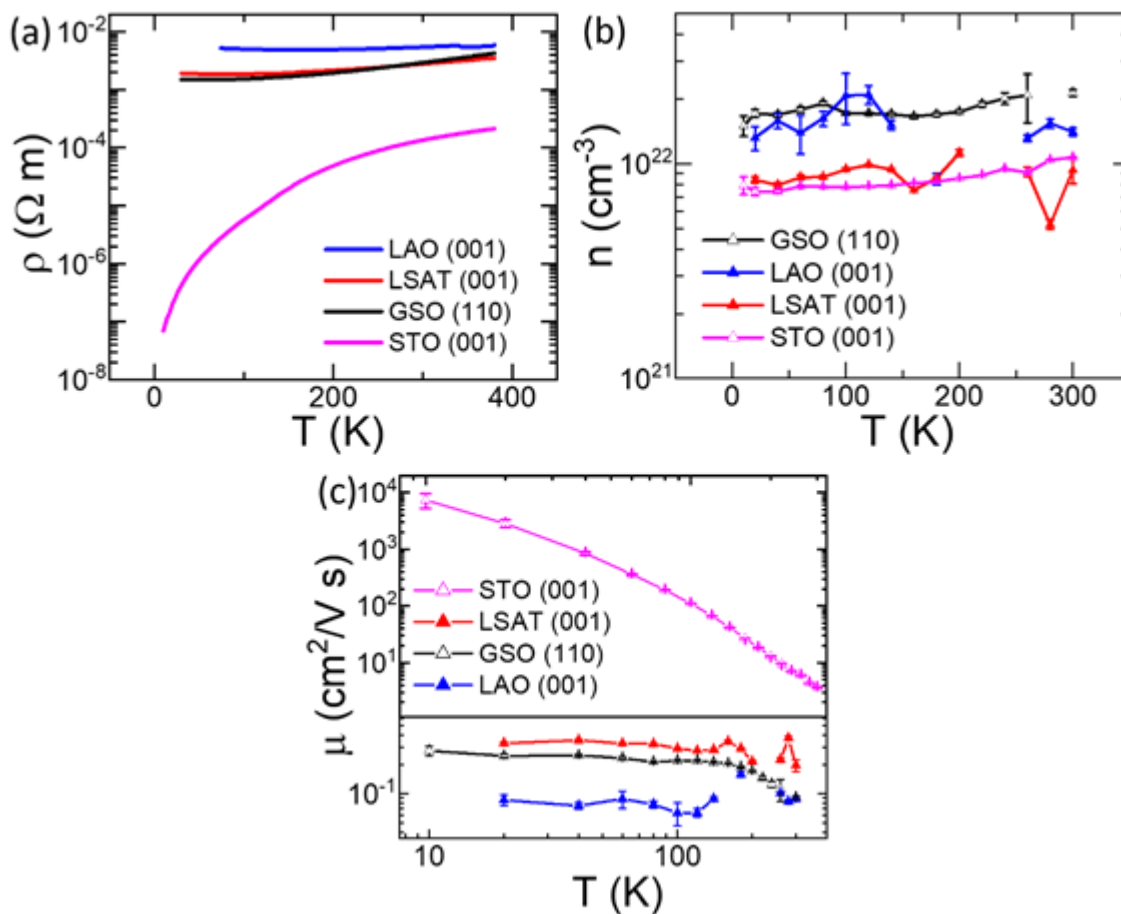


Figure 2. Substrate materials dependent Hall measurements for LSTO films grown at 5×10^{-4} Torr of oxygen. (a) Resistivity vs. temperature (ρ - T) where the strain along the c -axis is indicated accordingly, (b) Carrier concentration vs. temperature (n - T), (c) Mobility vs. temperature (μ - T) for these films on different substrates.

Auth

We have varied the oxygen pressure during the growth of LSTO films on STO and observed the effects on conductivity. **Figure 3** shows the Hall measurement results of LSTO films on STO grown at different oxygen partial pressure. It has been reported that oxygen partial pressure during the film growth has a strong effect on the overall resistivity of the materials studied.^[3, 5, 15, 18, 20, 21, 23, 27] Our results showed the similar trend. Specifically, samples grown at an oxygen pressures higher than 5×10^{-4} Torr shows a higher resistivity than samples grown at lower oxygen pressures (Figure 3a). For example, the LSTO film (grown at 5×10^{-4} Torr) on STO exhibits a resistivity of $\rho \sim 2 \times 10^{-5} \Omega \text{ cm}$ at room temperature, which are two orders of magnitude lower than that of the sample grown at 5×10^{-3} Torr. The temperature dependent carrier density and mobility shown in Figs. 3(b) and 3(c) demonstrated that both decreased carrier concentration and mobility with increasing oxygen pressure during film growth could contribute to the increased resistivity at given temperature. However, the significantly reduced carrier concentration dominates the increased resistivity at higher temperature because the mobility is not dramatically affected by changing the oxygen pressure during the film growth. At lower temperature such as 10 K, however, the mobility can still show one magnitude difference resulted from the oxygen pressure used in our experiments. This is reasonable since high oxygen partial pressure reduces the OV concentration as well as the OV related carriers. One could clearly use such a strategy, i.e., oxygen pressure during film growth, to manipulate the carrier mobility and concentration, and therefore the effective conductivity of the heterostructure stack.

Figure 3d shows the optical photos of bare STO substrates treated under the similar growth conditions used for the LSTO film growth and the LSTO/STO heterostructures with different LSTO film thickness. These bare STO substrates were annealed in an oxygen pressure of 5×10^{-4} Torr and a temperature of 700 or 750 °C for 30 min. As can be seen from the photos, annealed STO substrates under such conditions are still transparent and transport measurements confirm the insulating behavior from both treated substrates. We, however, have found that STO substrate changes to gray/blue color

when the annealing is carried out in an oxygen pressure of 5×10^{-4} Torr at a temperature above 800 °C. These experimental results clearly illustrated that an annealing of STO in a reducing environment (5×10^{-4} Torr, 700-750 °C, 30 min) alone is not sufficient to change a transparent and highly insulating STO substrate to conductive and/or different color. However, the LSTO/STO stacks with 28 nm and 122 nm LSTO show distinct light blue and dark blue color. As LSTO film has a bandgap of about ~ 3.72 eV (**Figure S2**, Tauc plot and photos of LSTO film on MgO) and is transparent, the blue color of LSTO/STO stacks should come from reduced STO substrate. Our results are consistent with reported color changes of reduced STO.^[39] We therefore propose that growing an oxygen deficient oxide layer on top of STO in a suitable reducing environment can promote oxygen transfer from STO substrate to the oxygen deficient film. This is consistent with the oxygen sponge effect, which shows STO substrate can be a source of oxygen for oxide films grown at low oxygen pressure.^[28] Therefore, we propose that STO substrate surface, contacting with the oxide film, suffers from a redox process during the oxide film growth in an oxygen deficient environment. This redox process produces a thin surface layer right on the top of STO substrate that is oxygen deficient and highly conductive. Laser plume has also been reported to reduce the STO substrate during PLD process and make the STO more conductive.^[26] To exclude such an effect in our case, we grew Au films under the same growth condition (as outlined above) on STO substrates. The STO substrates as shown in Figure 3d, after removing the Au film, are insulating and transparent. Therefore, the exposure to the laser plume during the film growth has a minor effect in our case. This designed experiment also supports our hypothesis that the growth of oxide films in a reducing environment pulls oxygen from STO substrates, while the growth of a non-oxide stable metal film such as Au and annealing alone at the same growth conditions do not induce oxygen transfer from STO substrate.

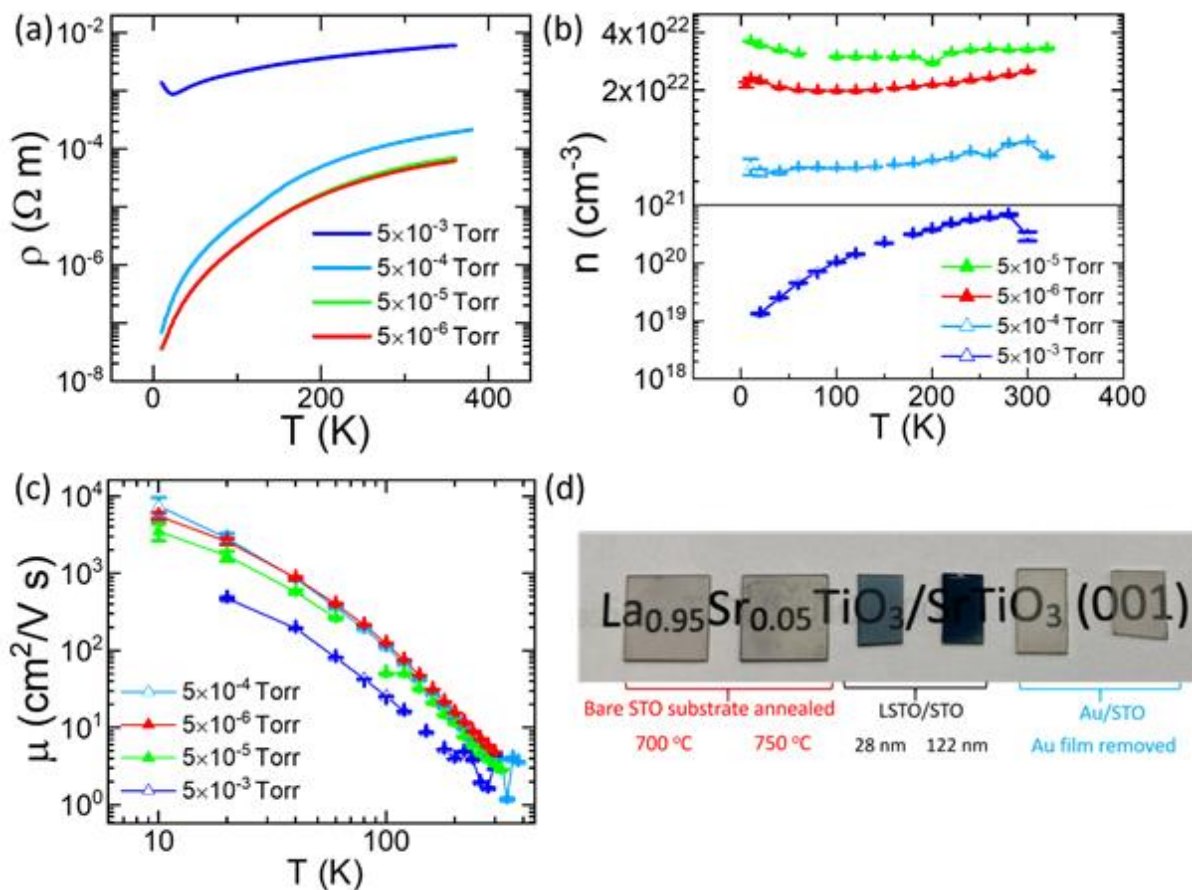
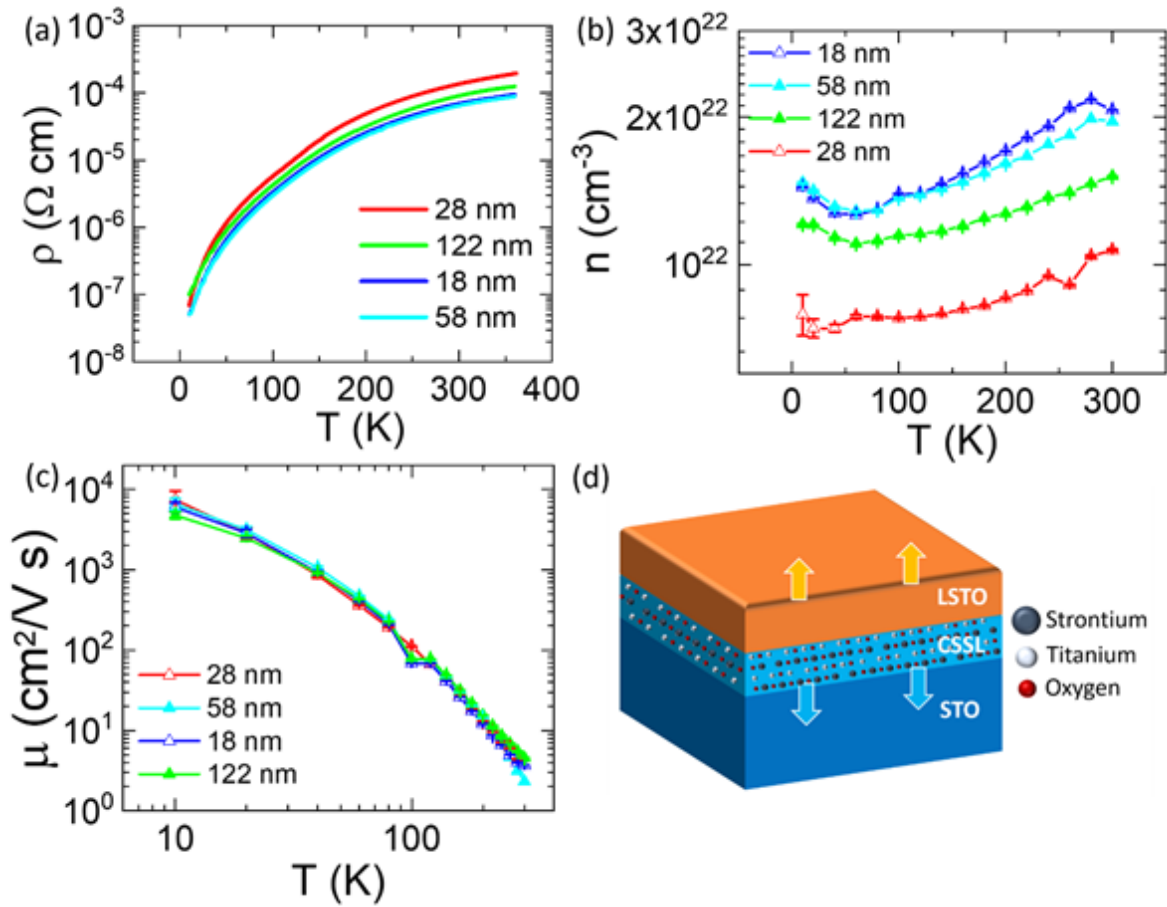


Figure 3. Temperature dependent (a) resistivity, (b) carrier concentration, and (c) mobility of LSTO films on STO grown in different oxygen partial pressure. (d) Photos of bare STO substrates (left two square samples) annealed in oxygen ($<5 \times 10^{-4}$ Torr) at 700 °C and 750 °C, LSTO/STO heterostructures (middle two dark color samples), and Au/STO heterostructures after removing Au films.

Auti

To explore the effect of LSTO layer thickness on the formation of conducting substrate surface layer (CSSL), LSTO/STO heterostructures with different LSTO thickness have been grown and measured. **Figure 4a** shows that ρ -T curves of films ranging from 18 nm to 122 nm. It is seen that the ρ -T curves are not a strong function of film thickness. If the STO substrate is highly resistive or the resistivity of the LSTO film is far smaller than that of the substrate, one could simply conclude that the film layer contributes to the measured conductivity. In our case, the experimental results have shown that the STO substrate, subjected to a thermal cycle at high temperature in a low oxygen pressure, exhibits a much lower resistivity which is 2-4 magnitude lower than that of LSTO films. Therefore, the ρ -T curves shown in Figure 4a should be controlled by the CSSL in STO. To show the LSTO thickness independent conductivity of the LSTO/STO heterostructures, the CSSL must also increase in thickness with the thickness of LSTO films (Figure 4b/4c). As we have discussed earlier, the LSTO film grown on STO in a relative low oxygen pressure can pull oxygen out from the STO and leaves oxygen vacancies in STO substrate. It is expected that the CSSL thickness increases with growing thicker LSTO layer as it creates more oxygen vacancies near STO interface. As schematically illustrated in Figure 4d, the CSSL increases in thickness when the LSTO film grows thicker. Understanding the existence and the origin of this CSSL becomes relevant since STO substrate offers the ability to provide oxygen to oxidize the film during the growth in low oxygen pressures.^[19, 27, 28] As one of the most commonly used substrates for the growth of multifunctional complex metal oxide films, STO itself could be responsible for many other reported exotic phenomena.

Figure 4. Temperature dependent (a) resistivity, (b) carrier concentration, and (c) mobility of LSTO/STO stacks with different LSTO film thickness. (d) An illustration of increasing the CSSL with increasing film thickness.



3. Conclusion

This article is protected by copyright. All rights reserved.

In this study, we have examined the effects of substrate materials, film thickness, and oxygen pressure for LSTO films to isolate the contributions of LSTO film, film-substrate interface, and substrate on the conductivity of the heterostructures. LSTO/STO stack shows the highest mobility and lowest resistivity compared to LSTO on other substrates. The formation of an oxygen-vacancy rich layer near the top region of STO substrate, driven by the growth of an oxide layer at given conditions rather than the growth condition alone, contributes to the enhanced conductivity of the LSTO/STO heterostructures. Such a surface layer is not achieved by annealing or the growth of Au layer alone at the same reducing condition. Our work provides an alternative physical origin of STO reduction during thin film growth and the mechanisms on oxygen transfer dynamics revealed here can be applied to design growth and functionalities of other heterostructures.

4. Experimental Section

Pulse laser deposition (PLD) was used to grow epitaxial LSTO thin films with different thicknesses on (001) STO, (110) GdScO₃ (GSO), (001) LAO, (001) LSAT, and CeO₂ buffered (001) STO substrates. To compare the degree of lattice strain of LSTO films on different substrates, we performed XRD and reciprocal space map (RSM) of the films. TEM and HRTEM was used to evaluate the interface and diffraction patterns of 28 and 122 nm LSTO/STO heterostructures. Temperature dependent carrier concentration (n vs T), mobility (μ vs T), and resistivity (ρ vs T) were measured from 10 K to 300 K with a magnetic field of 4 Tesla. Further detailed growth and characterization can be found from the Supporting Information.

Supporting Information

This article is protected by copyright. All rights reserved.

Supporting Information is available from the Wiley Online Library or from the author.

Acknowledgment

Z.C. and H.H.H. contributed to this work equally. The work at Los Alamos National Laboratory was supported by the NNSA's Laboratory Directed Research and Development Program, and Institute of Materials Science and was performed, in part, at the CINT, an Office of Science User Facility operated for the U.S. Department of Energy Office of Science. Los Alamos National Laboratory, an affirmative action equal opportunity employer, is managed by Triad National Security, LLC for the U.S. Department of Energy's NNSA, under contract 89233218CNA000001. The work at University at Buffalo was partially supported by the U.S. National Science Foundation under award number ECCS-1902623. Q. X. J. also acknowledges the CINT User Program.

Received: ((will be filled in by the editorial staff))

Revised: ((will be filled in by the editorial staff))

Published online: ((will be filled in by the editorial staff))

This article is protected by copyright. All rights reserved.

References

- [1] A. Chen, Q. Su, H. Han, E. Enriquez, Q. Jia, *Adv Mater* **2019**, 31, 1803241.
- [2] D. G. Schlom, L.-Q. Chen, C. J. Fennie, V. Gopalan, D. A. Muller, X. Pan, R. Ramesh, R. Uecker, *MRS Bulletin* **2014**, 39, 118.
- [3] F. Trier, D. V. Christensen, N. Pryds, *Journal of Physics D: Applied Physics* **2018**, 51.
- [4] X. Lu, A. Chen, Y. Luo, P. Lu, Y. Dai, E. Enriquez, P. Dowden, H. Xu, P. G. Kotula, A. K. Azad, D. A. Yarotski, R. P. Prasankumar, A. J. Taylor, J. D. Thompson, Q. Jia, *Nano Lett* **2016**, 16, 5751.
- [5] S. Gariglio, M. Gabay, J. M. Triscone, *APL Materials* **2016**, 4.
- [6] K. Zou, S. Ismail-Beigi, K. Kisslinger, X. Shen, D. Su, F. J. Walker, C. H. Ahn, *APL Materials* **2015**, 3.
- [7] E. N. Jin, L. Kornblum, D. P. Kumah, K. Zou, C. C. Broadbridge, J. H. Ngai, C. H. Ahn, F. J. Walker, *APL Materials* **2014**, 2.
- [8] J. Biscaras, N. Bergeal, S. Hurand, C. Grossetete, A. Rastogi, R. C. Budhani, D. LeBoeuf, C. Proust, J. Lesueur, *Phys Rev Lett* **2012**, 108, 247004.
- [9] J. Son, P. Moetakef, J. M. LeBeau, D. Ouellette, L. Balents, S. J. Allen, S. Stemmer, *Applied Physics Letters* **2010**, 96.
- [10] J. Biscaras, N. Bergeal, A. Kushwaha, T. Wolf, A. Rastogi, R. C. Budhani, J. Lesueur, *Nat Commun* **2010**, 1, 89.
- [11] S. Okamoto, A. J. Milli, *Nature* **2004**, 428, 630.
- [12] M. Choi, A. B. Posadas, C. A. Rodriguez, A. O'Hara, H. Seinige, A. J. Kellock, M. M. Frank, M. Tsoi, S. Zollner, V. Narayanan, A. A. Demkov, *Journal of Applied Physics* **2014**, 116.
- [13] R. Ghosh, D. Basak, S. Fujihara, *Journal of Applied Physics* **2004**, 96, 2689.
- [14] F. J. Wong, S.-H. Baek, R. V. Chopdekar, V. V. Mehta, H.-W. Jang, C.-B. Eom, Y. Suzuki, *Physical Review B* **2010**, 81.
- [15] W. Siemons, G. Koster, H. Yamamoto, W. A. Harrison, G. Lucovsky, T. H. Geballe, D. H. Blank, M. R. Beasley, *Phys Rev Lett* **2007**, 98, 196802.
- [16] R. Ohtsuka, M. Matvejeff, K. Nishio, R. Takahashi, M. Lippmaa, *Applied Physics Letters* **2010**, 96.

- [17] B. Vilquin, T. Kanki, T. Yanagida, H. Tanaka, T. Kawai, *Applied Surface Science* **2005**, 244, 494.
- [18] Z. Q. Liu, W. Lu, S. W. Zeng, J. W. Deng, Z. Huang, C. J. Li, M. Motapothula, W. M. Lü, L. Sun, K. Han, J. Q. Zhong, P. Yang, N. N. Bao, W. Chen, J. S. Chen, Y. P. Feng, J. M. D. Coey, T. Venkatesan, Ariando, *Advanced Materials Interfaces* **2014**, 1.
- [19] C. W. Schneider, M. Esposito, I. Marozau, K. Conder, M. Doebeli, Y. Hu, M. Mallepell, A. Wokaun, T. Lippert, *Applied Physics Letters* **2010**, 97.
- [20] B. I. Edmondson, S. Liu, S. Lu, H. W. Wu, A. Posadas, D. J. Smith, X. P. A. Gao, A. A. Demkov, J. G. Ekerdt, *Journal of Applied Physics* **2018**, 124.
- [21] A. Kalabukhov, R. Gunnarsson, J. Börjesson, E. Olsson, T. Claeson, D. Winkler, *Physical Review B* **2007**, 75.
- [22] W. S. Choi, S. Lee, V. R. Cooper, H. N. Lee, *Nano Lett* **2012**, 12, 4590.
- [23] B. Vilquin, T. Kanki, T. Yanagida, H. Tanaka, T. Kawai, *Solid State Communications* **2005**, 136, 328.
- [24] C. C. Hays, J.-S. Zhou, J. T. Markert, J. B. Goodenough, *Physics Review B* **1999**, 60.
- [25] F. V. E. Hensling, C. Xu, F. Gunkel, R. Dittmann, *Sci Rep* **2017**, 7, 39953.
- [26] F. V. E. Hensling, D. J. Keeble, J. Zhu, S. Brose, C. Xu, F. Gunkel, S. Danylyuk, S. S. Nonnenmann, W. Egger, R. Dittmann, *Sci Rep* **2018**, 8, 8846.
- [27] A. Sambri, D. V. Cristensen, F. Trier, Y. Z. Chen, S. Amoruso, N. Pryds, R. Bruzzese, X. Wang, *Applied Physics Letters* **2012**, 100.
- [28] K. T. Kang, B. Zhang, Y. Sharma, B. Paudel, H. Wang, P. Dowden, A. Chen, *Applied Physics Letters* **2020**, 117.
- [29] A. Spinelli, M. A. Torija, C. Liu, C. Jan, C. Leighton, *Phys Rev B* **2010**, 81.
- [30] J. S. Kim, S. S. A. Seo, M. F. Chisholm, R. K. Kremer, H. U. Habermeier, B. Keimer, H. N. Lee, *Physical Review B* **2010**, 82.
- [31] D. Kan, T. Terashima, R. Kanda, A. Masuno, K. Tanaka, S. Chu, H. Kan, A. Ishizumi, Y. Kanemitsu, Y. Shimakawa, M. Takano, *Nature Materials* **2005**, 4, 816.
- [32] X. Zhou, Z. Liu, *J Phys Condens Matter* **2021**, 33.
- [33] T. T. Zhang, C. Y. Gu, Z. W. Mao, X. F. Chen, Z. B. Gu, P. Wang, Y. F. Nie, X. Q. Pan, *Applied Physics Letters* **2019**, 115.
- [34] J. E. Sunstrom, S. M. Kauzlarich, P. Klavins, *Chemical Materials* **1992**, 4, 346.
- [35] L. Fan, X. Gao, D. Lee, E. J. Guo, S. Lee, P. C. Snijders, T. Z. Ward, G. Eres, M. F. Chisholm, H. N. Lee, *Adv Sci (Weinh)* **2017**, 4, 1700045.
- [36] H. H. Sung, J. T. Tsai, C. H. Lin, S. Y. Chen, J. C. Fan, C. R. Lin, *Materials Science Forum* **2011**, 700, 41.
- [37] Y. Tokura, Y. Taguchi, Y. Okada, Y. Fujishima, T. Arima, K. Kumagai, Y. Iye, *Phys Rev Lett* **1993**, 70, 2126.
- [38] D. W. Reagor, V. Y. Butko, *Nat Mater* **2005**, 4, 593.
- [39] M. L. Scullin, J. Ravichandran, C. Yu, M. Huijben, J. Seidel, A. Majumdar, R. Ramesh, *Acta Materialia* **2010**, 58, 457.

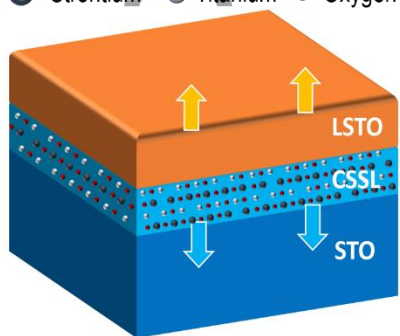
The Role of Oxygen Transfer in Oxide Heterostructures on Functional Properties

Zachary Corey, Henry H. Han, Kyeong Tae Kang, Xuejing Wang, Rebecca A. Lalk, Binod Paudel, Pinku Roy, Yogesh Sharma, Jinkyoun Yoo, Quanxi X. Jia, * Aiping Chen *

Table of Contents Summary:

This work reveals the key role of oxygen transfer from the substrate to the oxide layer resulting in a substrate surface conducting layer. Such an oxygen transfer process could play a significant role in functional properties of oxide heterostructures in general.

● Strontium ● Titanium ● Oxygen



Author Mail